

## *In Vivo* Response of Laser Processed Porous Titanium Implants for Load-Bearing Implants

AMIT BANDYOPADHYAY, ANISH SHIVARAM, SOLAIMAN TARAFDER, HIMANSHU SAHASRABUDHE,  
DISHARY BANERJEE, and SUSMITA BOSE

W. M. Keck Biomedical Materials Research Laboratory, School of Mechanical and Materials Engineering, Washington State University, Pullman, WA 99164-2920, USA

(Received 29 January 2016; accepted 2 June 2016; published online 15 June 2016)

Associate Editor Amir Abbas Zadpoor oversaw the review of this article.

**Abstract**—Applications of porous metallic implants to enhance osseointegration of load-bearing implants are increasing. In this work, porous titanium implants, with 25 vol.% porosity, were manufactured using Laser Engineered Net Shaping (LENS™) to measure the influence of porosity towards bone tissue integration *in vivo*. Surfaces of the LENS™ processed porous Ti implants were further modified with TiO<sub>2</sub> nanotubes to improve cytocompatibility of these implants. We hypothesized that interconnected porosity created *via* additive manufacturing will enhance bone tissue integration *in vivo*. To test our hypothesis, *in vivo* experiments using a distal femur model of male Sprague–Dawley rats were performed for a period of 4 and 10 weeks. *In vivo* samples were characterized *via* micro-computed tomography (CT), histological imaging, scanning electron microscopy, and mechanical push-out tests. Our results indicate that porosity played an important role to establish early stage osseointegration forming strong interfacial bonding between the porous implants and the surrounding tissue, with or without surface modification, compared to dense Ti implants used as a control.

**Keywords**—Additive manufacturing, LENS™, Porous Ti, TiO<sub>2</sub> Nanotubes, Osseointegration.

### INTRODUCTION

Titanium and its alloys have been established as one of the most desirable materials for load-bearing implants. The main reasons to use Ti implants are due to excellent corrosion resistance, good biocompatibility, high strength to weight ratio and resistance to fatigue

deformation. Even with excellent material properties, Ti-based load-bearing implants such as hip and knee prosthesis fail in large numbers (~600,000 knee replacement surgeries as of 2011) within the first 15 years.<sup>10</sup> Among others, interfacial instability and aseptic loosening have been identified as some of the key reasons for implant failure.<sup>38</sup> More specifically, failure of load-bearing implants can be grouped into three broad categories: (1) poor interfacial bonding between the implant surface and bone-tissue; (2) stress shielding due the mismatch in modulus between the implant and bone (~110–120 GPa for Ti alloys and 10–30 GPa for human cortical bone) and (3) wear induced osteolysis caused by to the excessive release of metal ions surrounding the bone-implant area. Ideally, the *in vivo* life of an implant can be improved by increasing the interfacial bond between the implant surface and the bone-tissue area, and reducing the effective modulus of the implant material.<sup>38</sup> It is possible to accomplish both by incorporating a porous metal coating on load-bearing implant surfaces. Effective modulus can be reduced by using porous materials, which also helps improve biological fixation *via* bone ingrowth through pores.<sup>21,23,38</sup> Such improvements of osseointegration properties for porous titanium materials have been shown through various *in vivo* results.<sup>17,20,22,24–26</sup>

Another known method to improve bonding at the bone-implant interface is to modify the implant surface topography at a nanostructural level to further facilitate the process of early stage osseointegration (bonding between the bone and surface of the implant). Rough surfaces tend to favor osteoblast proliferation, adhesion and mineralization compared to

Address correspondence to Amit Bandyopadhyay, W. M. Keck Biomedical Materials Research Laboratory, School of Mechanical and Materials Engineering, Washington State University, Pullman, WA 99164-2920, USA. Electronic mail: amitband@wsu.edu

non-modified surfaces.<sup>17,19</sup> *In vitro* and *in vivo* results have shown better surface adhesion and bone bonding ability for modified surfaces. One of the most common ways to modify the surface of titanium at nanostructural level is by growing TiO<sub>2</sub> nanotubes using electrochemical anodization method.<sup>7,17–19</sup> This method has gained popularity over the years due to its simple setup, and flexibility towards controlling the parameters of nanotubes. TiO<sub>2</sub> nanotubes, due to its nanomorphology, improve cell-materials interactions at the surface thereby improving the bonding towards bone. Also, nanotubes help lower the contact angles at the surface to make it hydrophilic, which further improves early stage osseointegration.<sup>11</sup>

Porous metallic materials were fabricated in using conventional manufacturing techniques such as powder sintering.<sup>29,32</sup> The main disadvantage in using conventional method is inherent brittleness of the final product.<sup>29,31</sup> Also control on parameters such as pore shape and distribution is limited. This could play a significant role in the mechanical and biological properties. Porous metallic implants fabricated using conventional methods showed inferior mechanical properties such as fatigue strength due to localized stress concentrations at the pore walls.<sup>41</sup> Post-processing treatments, in the form of high temperature sintering, are also required for implants processed using conventional techniques.<sup>1,22,29,31,41</sup> Additive manufacturing may overcome the limitations presented by conventional techniques by providing better control on various pore parameters along with fabrication of parts with complex shape and geometry with improved mechanical properties. Due to these advantages, demand for additively manufactured porous metallic implants is increasing.<sup>4,5</sup> Laser based solid free form (SFF) techniques that uses a powder bed such as selective laser melting (SLM)<sup>27,40</sup> and direct laser sintering<sup>34,37</sup> have been used recently to fabricate porous metallic implants such as porous Ti structures for orthopedic applications.

Laser Engineered Net Shaping (LENS<sup>TM</sup>) is another SFF technique that does not use a powder bed to fabricate near net shaped metallic parts with complex geometries. In this work, we have used LENS<sup>TM</sup> to make porous Ti samples. The objective of this study was to understand the effects of porous titanium implants, with and without surface modification, towards interfacial bonding between the implant and the bone-tissue area when compared with dense implants. We hypothesize that interconnected porosity created *via* additive manufacturing will enhance bone tissue integration *in vivo* compared to dense implants. Male Sprague–Dawley rats were used for *in vivo* study for a period of 4 and 10 weeks. *In vivo* samples were characterized *via* micro-computed tomography (CT) and

histological imaging, scanning electron microscopy, and mechanical push-out tests.

## MATERIALS AND METHODS

### *Processing of Porous Ti Samples Using LENS<sup>TM</sup>*

A schematic of LENS<sup>TM</sup> system is shown in Fig. 1. To fabricate porous Ti rods of diameter 3.0 mm for *in vivo* studies, commercial CAD software was used to design a cylindrical file of diameter 2.30 mm and length of 75 mm. Porosity was created using partial melting of the powder with low power of the laser.<sup>36</sup> This CAD design was fed into the LENS<sup>TM</sup> motion control software and converted into tool path files. For the processing of the porous Ti rods, commercially pure titanium powder (ATI Powder Metals, Pittsburgh, PA, USA) with spherical particle size of 44–149  $\mu\text{m}$  and 99.99% purity was used. The substrate used was also a commercially pure (99.99% purity) titanium plate (President Titanium, Hanson, MA, USA) of thickness of 3 mm. The LENS<sup>TM</sup> system (Optomec Inc., Albuquerque, NM USA) used to process samples was equipped with a continuous wave 500 W Nd:YAG laser. To create porosity of more than 20%, different processing parameters were tried, as shown in Table 1. After each batch, samples were tested to measure volume % porosity. Based on the measured porosity, the process parameters were altered, if needed, to achieve a 25 vol.% porosity samples. Final processing conditions were—laser power of 280 W, and raster scanning speed between 60 and 80 cm/min. During the entire processing period, LENS<sup>TM</sup> chamber oxygen level was maintained at or below 10 ppm and monitored using an oxygen analyzer. After processing, rods were cut to make multiple samples between 5.0 and 5.5 mm in length. The outer layers of the LENS<sup>TM</sup> processed samples were lightly ground on wet 500 grit SiC paper. After cutting and grinding, samples were ultrasonically cleaned in 100% ethanol for 20 min, followed by a series of rinsing in deionized (DI) water and blow drying with warm air.

### *Nanotubes Formation*

TiO<sub>2</sub> nanotubes were grown on LENS<sup>TM</sup> fabricated porous Ti rods using electrochemical anodization method. Post-fabrication, the porous Ti rods were cleaned using an ultrasonicator with DI water and acetone. The anodization setup consisted of a beaker with 1% hydrofluoric acid (HF) as electrolyte, porous Ti rod as anode and a platinum foil as cathode suspended at either ends using platinum wires. A constant voltage of 20 V was applied using a DC power supply

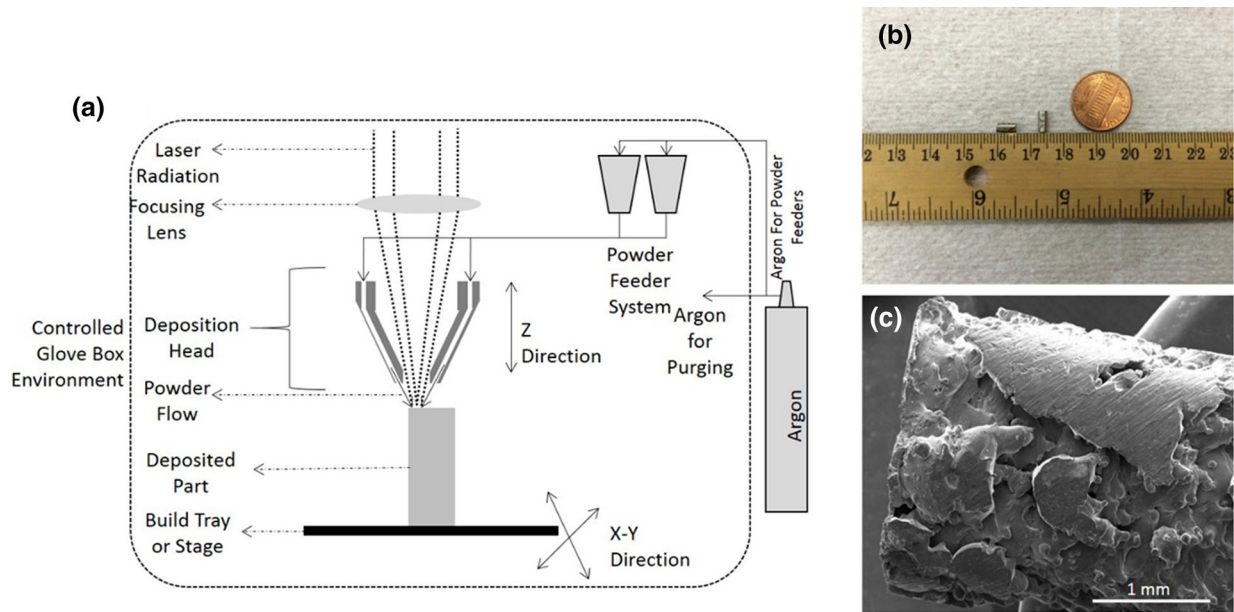


FIGURE 1. (a) Schematic representation of the LENS™ process. (b) LENS™ processed porous Ti samples with 25% porosity. (c) SEM image of the porous surface nature of LENS™ processed porous sample.

TABLE 1. Various processing parameters attempted for LENS™ processing of porous Ti rods.

| Sample  | Laser power (W) | Raster speed (cm/min) |       | Powder feed rate (g/min) | Porosity (%) |
|---------|-----------------|-----------------------|-------|--------------------------|--------------|
|         |                 | Contour               | Hatch |                          |              |
| Batch 1 | ~375            | ~100                  | ~100  | ~13.5                    | < 10         |
| Batch 2 | ~325            | ~76                   | ~81   | ~16                      | 10–12        |
| Batch 3 | ~325            | ~61                   | ~91   | ~18.5                    | 15–20        |
| Batch 4 | ~300            | ~61                   | ~81   | ~18.5                    | 15–20        |
| Batch 5 | ~280            | ~61                   | ~86   | ~20                      | ~25          |

(Hewlett Packard 0–60 V/0–50 A, 1000 W) throughout the process.<sup>33</sup> All samples were rinsed thoroughly using DI water. All the anodization experiments were performed at room temperature.

### In Vivo Study

#### Surgery and Implantation Procedure

A total of 12 male Sprague–Dawley rats weighing between 280 and 300 g were used for the study. All rats underwent bilateral surgery and Table 2 lists the details on number of implants and compositions used for the study. Prior to surgery, rats were housed in individual cages with alternating 12 h cycles of light and dark in temperature and humidity controlled rooms for acclimatization. Following acclimatization, rats were anesthetized using IsoFlo® (isoflurane, USP, Abbott Laboratories, North Chicago, IL, USA) coupled with an oxygen (Oxygen USP, A-L Compressed Gases Inc., Spokane, WA, USA) regulator, and

monitored by pedal reflex and respiration rate to maintain proper surgical anaesthesia. Using a drill bit, a defect in the distal femur was created similar to the diameter of the implant and the defect cavity was washed using saline solution to rinse out any remaining bone fragments. Following implantation, the incision was closed using synthetic absorbable surgical suture i.e., undyed braided coated VICRYL-polyglactin 910 (Ethicon Inc., Somerville, NJ, USA). Disinfectant in the form of Betadine solution was applied at the incision site post-surgery to prevent infection. No pain reduction or antibiotics were given prior to the surgery. Pain reduction *via* meloxicam injection was given post-surgery. At the end of 4 and 10 weeks post-surgery, rats were euthanized by overdosing the bell jar with isoflurane. The experimental and surgical procedure was performed according to a protocol approved by the Institutional Animal Care and Use Committee (IACUC) of Washington State University (Pullman, WA).

TABLE 2. Surgery details used for the *in vivo* study.

| Composition                                    | Time point | Number of rats |
|--|------------|----------------|
| Dense Ti (control)—right femur                 | 4 weeks    | 2              |
| Dense Ti (control)—left femur                  | 10 weeks   | 2              |
| Porous LENS™ Ti—right femur                    | 4 weeks    | 4              |
| Porous LENS™ Ti-NT (with nanotubes)—left femur | 10 weeks   | 4              |

### Push-Out Test and CT Scan Analysis

At necropsy, two sets of samples were harvested—one for push-out tests and CT scan analysis, and another set for histological analysis. A series of radiographic exposures of the bone samples (acquired using the X-ray energy source on the IVIS® Spectrum CT) were analyzed by computed tomography (CT) to generate a 3D volume. Scans were performed using a 40  $\mu\text{m}$  voxel size and 150  $\mu\text{m}$  (pixel size) resolution. Three-dimensional (3D) images of the defects were reconstructed from the scans by the Living Image® Software 4.4. Rat femur bones were provided to Scanco for high resolution micro CT imaging and analysis. Samples were scanned on a high-resolution, volumetric micro CT scanner ( $\mu\text{CT}40$ , Scanco Medical, Zurich, CH). The image data was acquired with the following parameters: 10  $\mu\text{m}$  isotropic voxel resolution at 300 ms exposure time, 1000 Projections per 180, and 1 frame/1 per view. Push-out tests were performed to determine the interfacial shear modulus between the tissue and the implant using a universal material testing machine (Instron, PA, USA) in compression using a 300 lb load cell. The shear modulus was calculated from the stress–strain plots of the push out test experiments.

### Histology and SEM Characterization

For histomorphological analysis, bone-implant samples were fixed in 10% formalin solution. Fixed samples were then dehydrated in series of ethanol (70, 95 and 100%), 1:1 ethanol–acetone mixture and finally 100% acetone. Following dehydration, samples were embedded in Spurr's resin, cut into thin sections ( $n = 3$  for each sample) using diamond blade, mounted on glass slides and stained using modified Masson Goldner's trichrome staining method.<sup>11</sup> Stained implant-tissue sections were then observed under light microscope (Olympus BH-2, Olympus America Inc., USA). Stained samples were then characterized under FES-EM (FEI Quanta 200, FEI Inc., OR, USA), which was maintained at low operating voltage of 10 kV and run under low vacuum.

## RESULTS

### Surface Morphology of LENS Processed Porous Ti Implants and Nanotubes

SEM images of LENS™ processed porous Ti rods, with and without anodization, are shown in Fig. 2. The volume porosity was approximately 25%. The pore size was found to be in the range of 200–300  $\mu\text{m}$ . From our previous studies, LENS™ processed porous Ti structures have Young's modulus in the range of 2–44 GPa<sup>5,38</sup> which is in the range of human cortical bone values of 7–30 GPa.<sup>38</sup> Also the mechanical strength for these porous structures tend to vary from 24 to 463 MPa.<sup>38</sup> Anodization of porous Ti samples resulted in TiO<sub>2</sub> nanotubes with diameter of  $105 \pm 30$  nm and length of  $375 \pm 35$  nm. The current range of parameters for nanotubes were concluded from our previous work, which showed TiO<sub>2</sub> nanotubes to be thermally stable, and also mechanically stable upon implantation *ex vivo*.<sup>33,34</sup>

### CT Scan and Push Out Test Analysis

CT scan analysis was performed for samples after 10 weeks to see the presence of any defects or gaps, and bonding around the implant which are shown in Fig. 3. The images from CT scans showed no defects around the implant and a good bonding was observed at the interface between the bone tissue and implant interface. Images also showed that the implants were properly lodged into the bone during surgery, which is also an important aspect. Porous samples showed better signs of bonding as compared to the dense samples. Lower resolution CT scan images showed good signs of bonding for porous samples, but could not provide sufficient information about the bone ingrowth into the pores. Thus, higher resolution scans were performed to observe the same. High resolution images of CT scans are shown in Fig. 4. These images clearly show osseointegration in the porous network for better bone-tissue bonding.

The interfacial shear modulus values resulting from the push out experiments are shown in Table 3. After



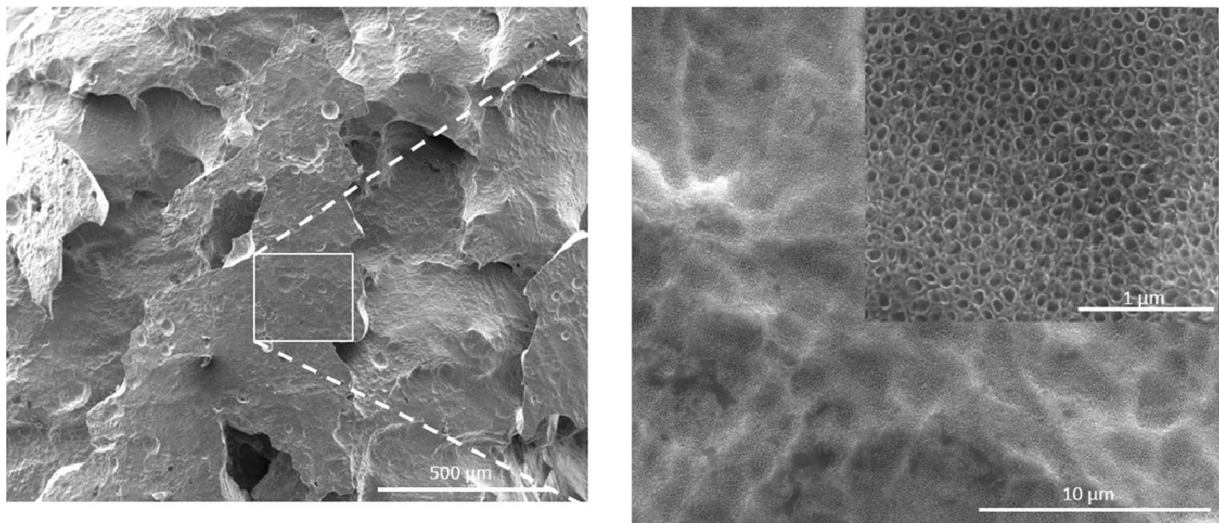


**FIGURE 2.** Porous Ti implant with fabrication of nanotubes with diameter  $105 \pm 30$  nm and length  $375 \pm 35$  nm using anodization method.

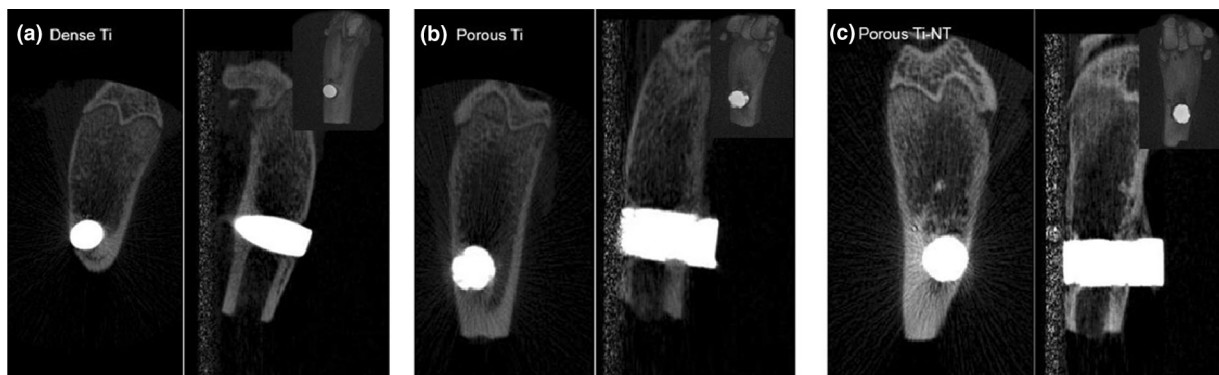


**FIGURE 3.** Computed tomography images of implants after 10 weeks showing proper lodging of the implant into the bone with no defects or gaps along with the implant-tissue bonding.

4 weeks, the interfacial shear modulus for porous samples is higher than the dense Ti samples, which indicates good signs of interfacial bonding between the implant and the tissue at early stages. After 10 weeks, bone fractured for all samples before the implant could be taken out. Therefore, all numbers look similar to the strength of the bone.

#### *Histological Evaluation*

Histological evaluation at the bone-implant interface was performed to understand the effect of porous surface with and without surface modification for biocompatibility and new bone formation at the end of 4 and 10 weeks. Figure 5 represents the histological evaluation of samples after 4 and 10 weeks for dense Ti, porous Ti and porous Ti with nanotubes. Signs of osteoid like new bone formation can be observed as early as 4 weeks. The orange-red region surrounding

the implant area represents the osteoid formation which indicates no cytotoxic effects due to implantation. The greenish area indicates the mineralized bone and the bluish black spots indicate the nuclei. Similar new bone like osteoid formation was observed at a greater extent for samples after 10 weeks. The osteoid formation can be seen almost completely surrounding the implant area with very few visible gaps. However osteoid formation in porous samples was more than control dense samples.

#### *SEM Characterization*

It could be observed from Figs. 6, 7 and 8, which shows the SEM images of dense Ti, porous Ti and porous Ti with nanotubes after 4 and 10 weeks, respectively. Histological evaluations showed signs of osteoid formation for all samples after 4 weeks and good early stage osteoid like new bone formation or

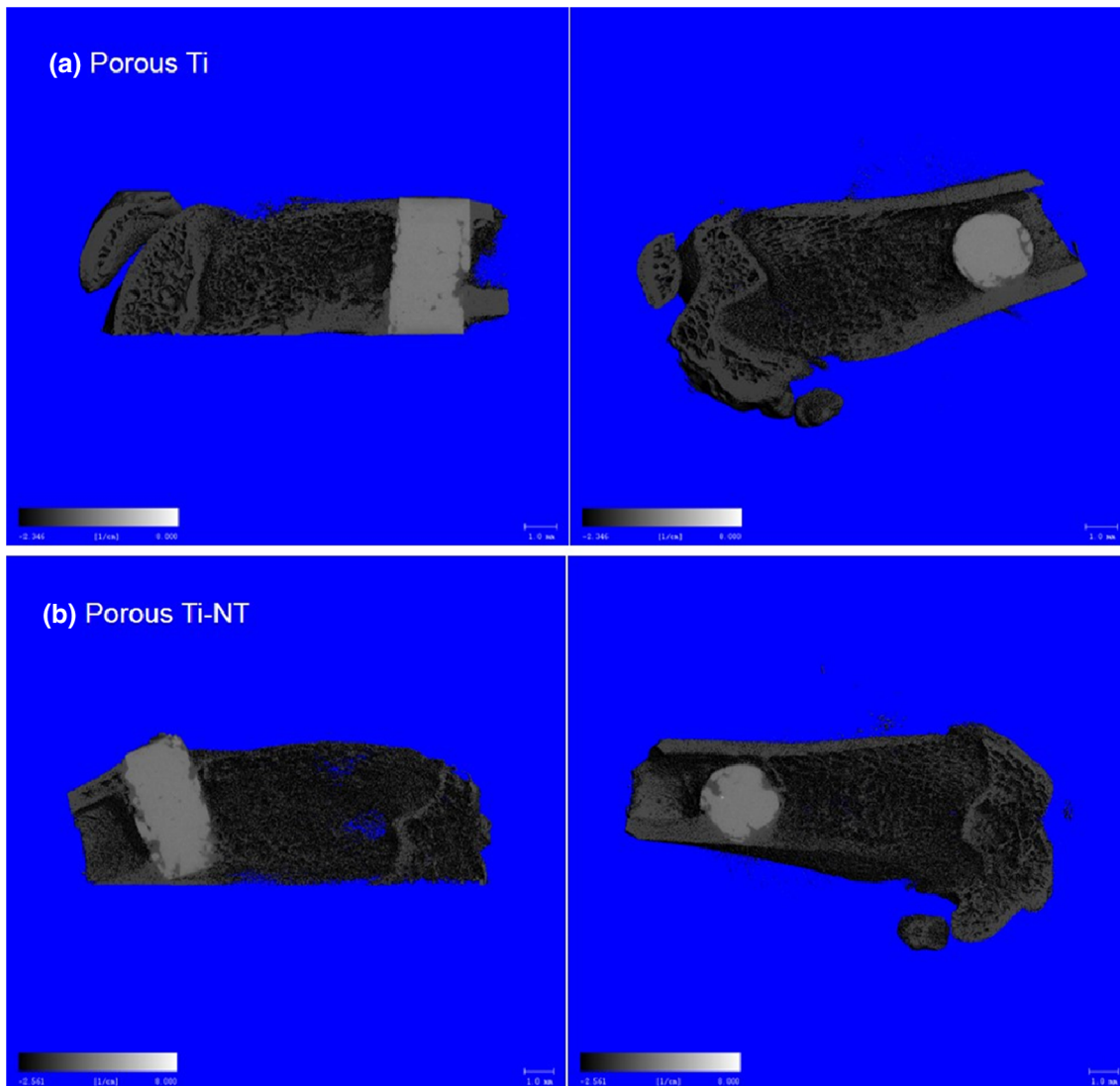


**FIGURE 4.** High resolution micro CT images showing good interfacial bonding between the porous implants with the tissue along with the bone ingrowth between the pores.

**TABLE 3.** Shear modulus values for each composition after 4 and 10 weeks respectively ( $n = 2$ ).

| Time point | Composition                     | Shear modulus (MPa) |
|------------|---------------------------------|---------------------|
| 4 Weeks    | Dense Ti                        | 14.865 $\pm$ 2.625  |
|            | LENS <sup>TM</sup> porous Ti    | 25.82 $\pm$ 1.94    |
|            | LENS <sup>TM</sup> porous Ti-NT | 29.38 $\pm$ 2.52    |
| 10 Weeks   | Dense Ti                        | 114.82 $\pm$ 6.99   |
|            | LENS <sup>TM</sup> porous Ti    | 117.78 $\pm$ 22.15  |
|            | LENS <sup>TM</sup> porous Ti-NT | 115.56 $\pm$ 0.30   |

osteogenesis after 10 weeks. As seen from Fig. 5, it is not clear how well the bonding between the tissue and the implant is for each composition. For a better idea on the bonding at the interface between the tissue and the implant, SEM images of the stained samples were obtained at the bone-tissue interface. Distinct gaps at

the interface between the tissue and the implant could be observed for all samples after 4 weeks. But the gap reduced as we move from dense Ti samples towards the porous samples and is considerably less for porous Ti samples with nanotubes. After 10 weeks, the gap at the interface is further reduced for porous samples

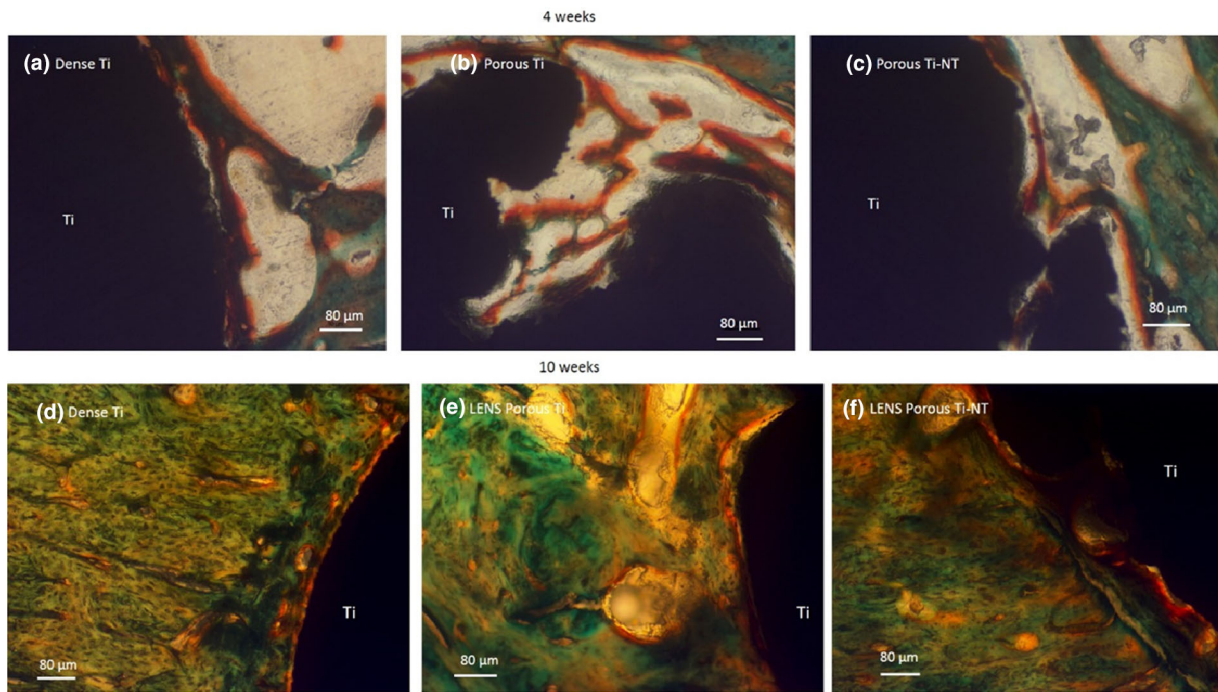


**FIGURE 5.** Photomicrograph showing the histology images after 4 weeks (a, b, c) and 10 weeks (d, e, f) where signs of osteoid like new bone formation could be seen in orange/red color. Modified Masson Goldner's trichrome staining method was used.

compared to dense Ti samples. Porous samples with nanotubes is showing negligible gap at the interface between the tissue and the implant. These results signify improved osseointegration between the bone tissue and the implant interface in which porous Ti samples showing improved bone bonding ability compared to the dense Ti samples.

## DISCUSSION

LENS<sup>TM</sup> is a powder based additive manufacturing technique that is capable of forming near net shaped metallic and metal-ceramic composite parts. Under the ASTM Standards for Terminologies for Additive Manufacturing, the LENS<sup>TM</sup> technique is categorized under direct energy based techniques.<sup>2</sup> The LENS<sup>TM</sup> system has two or more powder feeders through which powder is fed in a pressurized argon gas carrier bed. The powder feeding system is arranged in a way that the powder converges at the focal point of the laser beam. This incoming powder and the laser radiation meet on a stage or the substrate. As the powder absorbs the incident radiation, it melts and forms a small pool of molten metal or metal-ceramic mixture. The stage is capable of moving in the *X* and *Y* directions, and as the stage moves creating a liquid metal deposit along the path, the molten pool rapidly solidifies. Simultaneous movements of the stage in *X* and *Y* directions, and deposition

of the powder lead to “printing” of one layer of material. The laser focusing system and the powder delivery system move upwards in the *Z* direction once a layer deposition is done. The upward motion is controlled by the motion control software that ensures that the movement is equivalent to one layer thickness. Once the assembly moves up by one layer thickness, a second layer is deposited over the first layer. This layer-by-layer deposition sequence is continued until the complete part geometry is realized. The LENS<sup>TM</sup> deposition process is carried out in a glove box containing argon. The level of oxygen in the glove box is maintained at or below 10 ppm and is monitored throughout the build process. By simultaneously feeding two different powders from two different hoppers, alloying can be carried out *in situ*. The hoppers can also be used at different times in the process of building the same part and thus compositionally graded structures and multi-material structures can be fabricated.<sup>3,15</sup> The LENS<sup>TM</sup> build jobs are controlled using parameters such as laser power, raster scan speed and powder feed rate. These parameters can be altered throughout the process as required. By careful alteration of these parameters, components with different powder input and thus with different solidification rates can be formed. This can lead to the creation of thermally graded structures.<sup>9</sup>

The experimental procedures discussed in this research demonstrate the ability to fabricate porous titanium implants with random porosity using



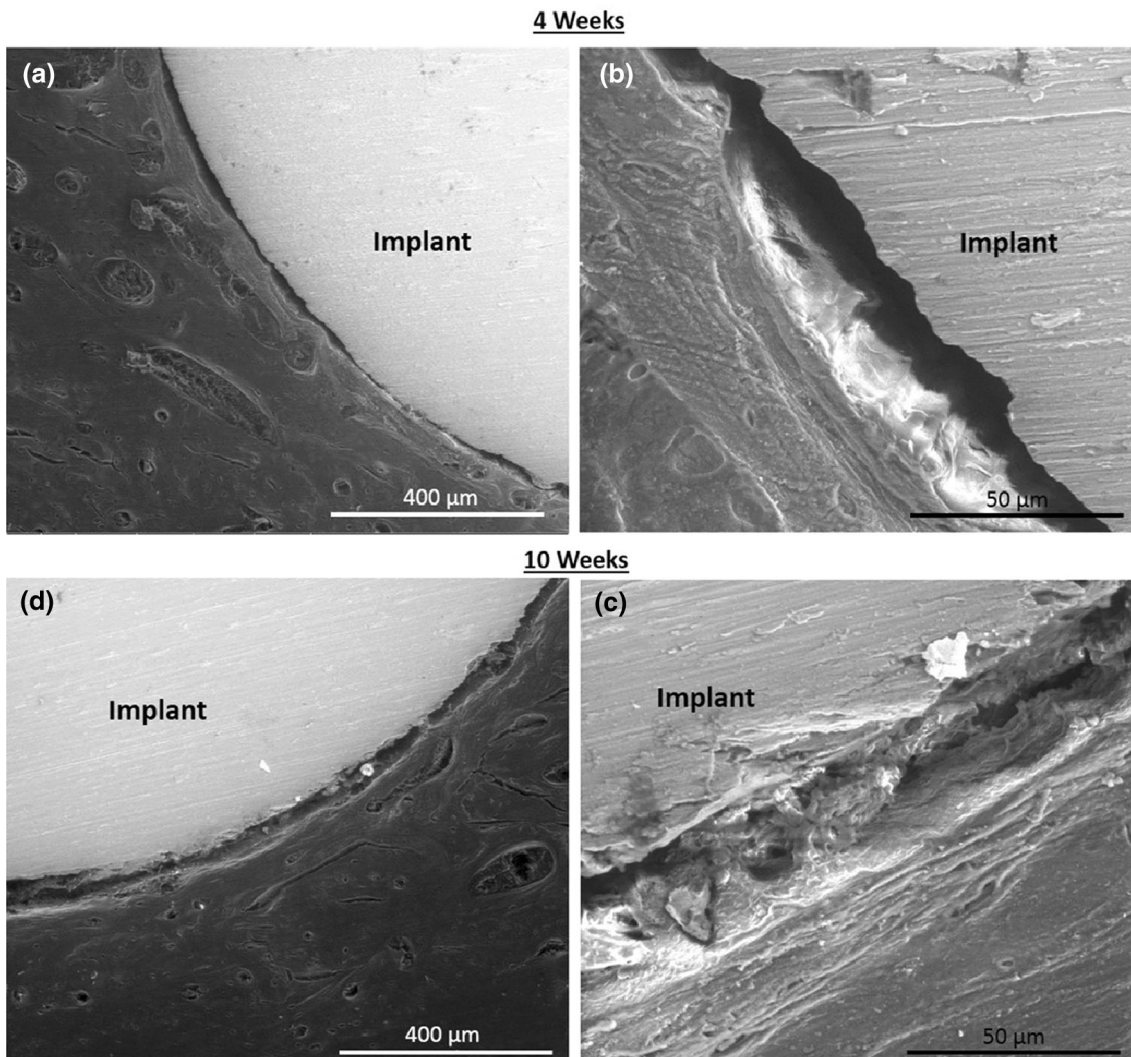


**FIGURE 6.** SEM images of stained dense Ti samples after 4 (a, b) and 10 (c, d) weeks showing the interfacial bonding between the implant and the tissue.

LENS<sup>TM</sup> to mimic the properties of human bone. The optimal porosity requirement for an implant material to be effective should be more than 20%.<sup>36</sup> Based on this requirement and considering the porous nature of bone material, these porous implants were fabricated. Porous structures with an optimal pore size of greater than 200 μm plays an important role in enabling the capillary tissue and migration of osteoprogenitor cells into the pores which lowers the density of the metal implants and helps in reducing the mismatch and stiffness between the implant and the bone-tissue area.<sup>4,22,23</sup> Moreover, mechanical properties like Young's modulus and compressive strength of these laser processed porous samples can also be tailored to match that of human cortical bone to increase the implant life *in vivo*.<sup>4,5,23</sup>

*In vivo* study using male Sprague–Dawley rats was performed for 4 and 10 weeks to measure bone tissue

integration. Computed tomography analysis was performed on samples after 10 weeks to see the bonding between the implant and tissue, and also the possible bone ingrowth in porous samples. CT scan revealed no major defects or gaps around the implants. Porous samples showed better bone-tissue integration compared to dense samples. High resolution images of CT scan of the porous implants along with the bone revealed better bonding of porous implants with the tissue. Bone ingrowth into the pores of the implant could be observed in the high resolution CT scan images. Porous samples with nanotubes particularly showed better bone tissue integration which could be seen from both the views of the sample images. CT scan analysis is one good way to analyze the samples in a non-destructive manner but is somehow limited in biomedical field mostly towards porous samples where porous



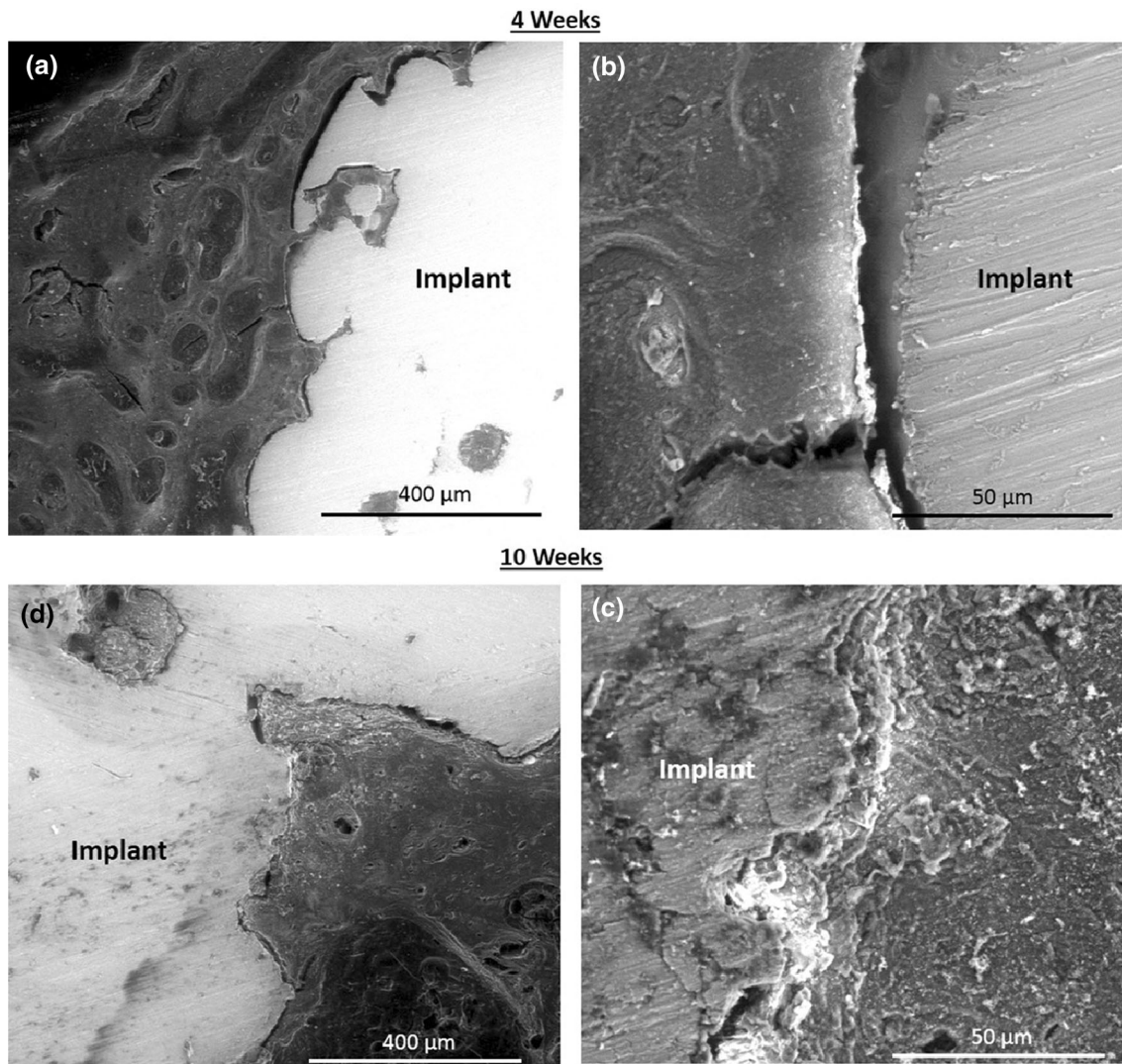


**FIGURE 7.** SEM images of stained porous Ti samples after 4 (a, b) and 10 (c, d) weeks showing the interfacial bonding between the implant and the tissue.

network needs to be characterized observing bone in growth in the pores.

Further analysis on the bone-tissue integration was done using the push out tests and results are given in Table 3. It can be noticed from the 4 weeks data that the interfacial shear moduli for porous samples are higher compared to the dense samples. Porous samples with nanotubes showed higher modulus overall due to better biocompatibility as the nanomorphology improves the surface properties thereby improving the bonding between the bone and the implant. For 10 weeks data, we see the values for all composition are in similar range. For all 10 weeks samples, bone broke as the samples were fully integrated. The ultimate shear strength of bone is in the range of 130–180 MPa, which was similar to the numbers we got from our experiment due to bone fracture.<sup>14,35,39</sup> It can

be concluded that the interfacial bonding between the implant and the tissue was too strong and exceeded the limit of bone strength due to which the final modulus value could not be obtained for 10 weeks samples. Previous studies also support our findings where similar experiments have been performed using porous metallic implants—push out tests (in compression) and pull out tests (in tension), and resulted in the fracture of the bone.<sup>6,8,12,13,25,28</sup>

One of the main objectives of this research was to promote early stage osseointegration through strong interfacial bonding between bone and implant surfaces with or without surface modification. Histological evaluation after 4 weeks showed better new bone formation for porous Ti samples than dense samples, where the osteoid like new bone formation could be seen forming around the open pores. After 10 weeks,

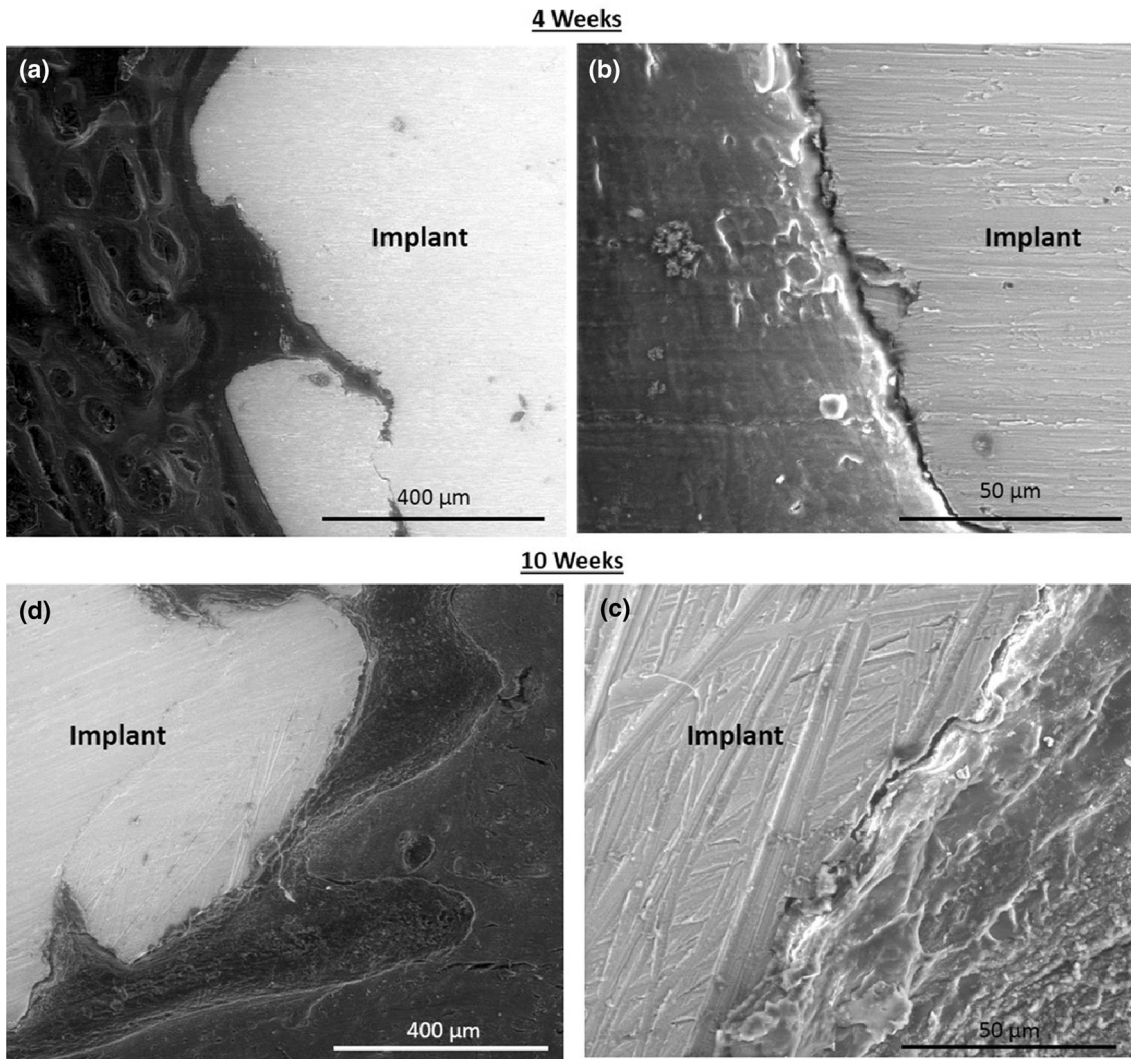


**FIGURE 8.** SEM images of stained porous Ti-NT samples after 4 (a, b) and 10 (c, d) weeks showing the interfacial bonding between the implant and the tissue.

the osteoid formation was seen to a greater extent in all samples. For porous samples, more osteoid formation could be seen near the porous surface. Porous surface tended to show improved biological fixation than dense samples. Porosity helps in inducing surface roughness which results in higher surface area and promotes better osteogenesis by new bone formation between the implant surface and the living tissue.<sup>16</sup> Surface morphology along with pore size, pore interconnectivity and pore volume promotes bone growth. The complete bone remodeling however takes a minimum of 12 weeks.<sup>21,30</sup> However in our case we could observe almost complete bone regeneration after 10 weeks in porous samples which confirmed enhanced early stage osseointegration. The SEM images of the stained samples after 4 weeks showed considerable gaps in dense Ti samples when compared with porous

samples. Better signs of bonding could be seen in porous samples to confirm almost complete bonding between the implant and the tissue with no gaps or incomplete bonding after 10 weeks. This signifies the importance of inducing porosity in implants towards bone growth. In fact, better interfacial bonding was seen in surface modified porous samples with nanotubes. Surface modification on a nanoscale level by growing  $\text{TiO}_2$  nanotubes further enhances the biocompatibility of the Ti surface thereby promoting better osteoconductive properties.  $\text{TiO}_2$  nanotubes help in increasing the surface roughness which results in higher surface area making the surface contact angle really low and the surface more hydrophilic to improve biocompatibility.<sup>7,17,19</sup> The hydrophilicity and increase in surface area improve the apatite formation on the surface making it more reactive and



osteconductive.<sup>17,19</sup> Cell adhesion also improves due to surface modification which results in better cell growth and stimulates its differentiation which results in a strong bonding between surface and the tissue.<sup>17,38</sup>

Presence of loosely attached and entrapped powder particles could be one of the issue which can result in dislodging from the implant and causing some sort of irritation which can be solved by simple mechanical treatment. Partial melting of powders is performed to induce porosity which generally results in strong interfacial bonding at particle interfaces due to liquid metal.<sup>4,5,38</sup> With the help of laser processed additively manufactured porous metallic implants, one can fabricate near net shaped parts with mechanical and biological properties similar to bone. One can also fabricate compositionally gradient structures with porous coating one side and a hard coating on the other side based on patient specific needs thereby improving the *in vivo* life of the implant.

## CONCLUSIONS

LENS<sup>TM</sup> was used to fabricate porous titanium implants with 25 vol.% porosity to study the effect of porous titanium implants on bone-tissue integration using a rat distal femur model. TiO<sub>2</sub> nanotubes were grown on the porous Ti surface using electrochemical anodization method to further enhance early stage osseointegration. Male Sprague–Dawley rats were used for the *in vivo* study for a period of 4 and 10 weeks. Shear modulus calculated from push out tests showed the highest value of ~30 MPa for surface modified porous titanium implants compared to ~15 MPa for dense Ti samples after 4 weeks showing early signs of osseointegration for surface modified porous titanium implants. However 10 weeks results showed fully integrated implants, which resulted in the fracture of the bone during testing. CT scan analysis revealed good bonding between the implants and the surrounding bone for porous implants with bone ingrowth being seen into the pores. Good signs of osseointegration with strong interfacial bonding at the implant-bone tissue interface were observed for porous implants especially ones with nanotubes in histological and SEM images. Based on our results, we can conclude that porous Ti implants, with and without surface modification, enhance early stage osseointegration. We can further conclude that surface modified porous Ti implants with TiO<sub>2</sub> nanotubes help defect healing *via* increasing the interfacial bonding between the implant and the bone.

## ACKNOWLEDGMENTS

The authors would like to thank Scanco USA, Inc. for their help with high resolution micro CT experiment and analysis. Research reported in this publication was also supported by the National Institute of Arthritis and Musculoskeletal and Skin Diseases of the National Institutes of Health under Award Numbers R01 AR067306-01A1 and R01 AR066361-01A1. The content is solely the responsibility of the authors and does not necessarily represent the official views of the National Institutes of Health.

## REFERENCES

- <sup>1</sup>Asaoka, K., N. Kuwayama, O. Okuno, *et al.* Mechanical properties and biomechanical compatibility of porous titanium for dental implants. *J. Biomed. Mater. Res.* 19(6):699–713, 1985.
- <sup>2</sup>ASTM Standard F2792-12a. Standard Terminology for Additive Manufacturing Technologies. West Conshohocken, PA: ASTM International, 2012, doi:10.1520/F2792-12A, <http://www.astm.org>.
- <sup>3</sup>Balla, V. K., W. Xue, S. Bose, *et al.* Functionally graded Co–Cr–Mo coating on Ti–6Al–4V alloy structures. *Acta Biomater.* 4(3):697–706, 2008.
- <sup>4</sup>Balla, V. K., W. Xue, S. Bose, *et al.* Engineered porous metals for implants. *JOM* 60(5):45–48, 2008.
- <sup>5</sup>Bandyopadhyay, A., V. K. Balla, W. Xue, *et al.* Application of laser engineered net shaping (LENS) to manufacture porous and functionally graded structures for load bearing implants. *J. Mater. Sci. Mater. Med.* 20(1):29–34, 2009.
- <sup>6</sup>Beaupied, H., E. Lespessailles, and C. L. Benhamou. Evaluation of macrostructural bone biomechanics. *Joint Bone Spine* 74(3):233–239, 2007.
- <sup>7</sup>Bjursten, L. M., L. Rasmusson, S. Oh, *et al.* Titanium dioxide nanotubes enhance bone bonding in vivo. *J. Biomed. Mater. Res. Part A* 92(3):1218–1224, 2010.
- <sup>8</sup>Bobyn, J. D., G. J. Stackpool, S. A. Hacking, *et al.* Characteristics of bone ingrowth and interface mechanics of a new porous tantalum biomaterial. *J. Bone Joint Surg. Br.* 81(5):907–914, 1999.
- <sup>9</sup>Bontha, S., N. W. Klingbeil, P. A. Kobryn, *et al.* Thermal process maps for predicting solidification microstructure in laser fabrication of thin-wall structures. *J. Mater. Process. Technol.* 178(1–3):135–142, 2006.
- <sup>10</sup>Bose, S., and A. Bandyopadhyay. Introduction to biomaterials. In: *Characterization of Biomaterials*, edited by A. Bandyopadhyay, and S. Bose. Waltham: Elsevier, 2013, pp. 1–9.
- <sup>11</sup>Bose, S., S. Tarafder, S. Banerjee, *et al.* Understanding in vivo response and mechanical property variation in MgO, SrO and SiO<sub>2</sub> doped  $\beta$ -TCP. *Bone* 48(6):1282–1290, 2011.
- <sup>12</sup>Brammer, K. S., S. Oh, C. J. Cobb, *et al.* Improved bone-forming functionality on diameter-controlled TiO<sub>2</sub> nanotube surface. *Acta Biomater.* 5(8):3215–3223, 2009.
- <sup>13</sup>Brånemark, R., L. O. Öhrnell, P. Nilsson, *et al.* Biomechanical characterization of osseointegration during



- healing: an experimental in vivo study in the rat. *Biomaterials* 18(14):969–978, 1997.
- <sup>14</sup>Burstein, A. H., D. T. Reilly, and M. Martens. Aging of bone tissue: mechanical properties. *J. Bone Joint Surg.* 58(1):82–86, 1976.
- <sup>15</sup>Collins, P. C., R. Banerjee, S. Banerjee, *et al.* Laser deposition of compositionally graded titanium–vanadium and titanium–molybdenum alloys. *Mater. Sci. Eng. A* 352(1): 118–128, 2003.
- <sup>16</sup>Cornell, C. N., and J. M. Lane. Current understanding of osteoconduction in bone regeneration. *Clin. Orthop.* 1(suppl. 355S):267–273, 1998.
- <sup>17</sup>Das, K., V. K. Balla, A. Bandyopadhyay, *et al.* Surface modification of laser-processed porous titanium for load-bearing implants. *Scripta Mater.* 59(8):822–825, 2008.
- <sup>18</sup>Das, K., S. Bose, and A. Bandyopadhyay. Surface modifications and cell–materials interactions with anodized Ti. *Acta Biomater.* 3(4):573–585, 2007.
- <sup>19</sup>Das, K., S. Bose, and A. Bandyopadhyay. TiO<sub>2</sub> nanotubes on Ti: influence of nanoscale morphology on bone cell–materials interaction. *J. Biomed. Mater. Res. Part A* 90(1):225–237, 2009.
- <sup>20</sup>Fujibayashi, S., M. Neo, H. M. Kim, T. Kokubo, *et al.* Osteoinduction of porous bioactive titanium metal. *Biomaterials* 25(3):443–450, 2004.
- <sup>21</sup>Hing, K. A., S. M. Best, K. E. Tanner, *et al.* Quantification on bone ingrowth within bone-derived porous hydroxyapatite implants of varying density. *J. Mater. Sci. Mater. Med.* 10(11):663–670, 1999.
- <sup>22</sup>Karageorgiou, V., and D. Kaplan. Porosity of 3D biomaterial scaffolds and osteogenesis. *Biomaterials* 26(27):5474–5491, 2005.
- <sup>23</sup>Krishna, B. V., S. Bose, and A. Bandyopadhyay. Low stiffness porous Ti structures for load-bearing implants. *Acta Biomater.* 3(6):997–1006, 2007.
- <sup>24</sup>Li, J. P., P. Habibovic, M. Van den Doel, *et al.* Bone ingrowth in porous titanium implants produced by 3D fiber deposition. *Biomaterials* 28(18):2810–2820, 2007.
- <sup>25</sup>Liebschner, M. A. Biomechanical considerations of animal models used in tissue engineering of bone. *Biomaterials* 25(9):1697–1714, 2004.
- <sup>26</sup>Lopez-Heredia, M. A., E. Goyenvalle, E. Aguado, *et al.* Bone growth in rapid prototyped porous titanium implants. *J. Biomed. Mater. Res. Part A* 85(3):664–673, 2008.
- <sup>27</sup>Mullen, L., R. C. Stamp, W. K. Brooks, *et al.* Selective laser melting: a regular unit cell approach for the manufacture of porous, titanium, bone in-growth constructs, suitable for orthopedic applications. *J. Biomed. Mater. Res. B Appl. Biomater.* 89(2):325–334, 2009.
- <sup>28</sup>Nishiguchi, S., H. Kato, H. Fujita, *et al.* Titanium metals form direct bonding to bone after alkali and heat treatments. *Biomaterials* 22(18):2525–2533, 2001.
- <sup>29</sup>Oh, I. H., N. Nomura, N. Masahashi, *et al.* Mechanical properties of porous titanium compacts prepared by powder sintering. *Scripta Mater.* 49(12):1197–1202, 2003.
- <sup>30</sup>Otsuki, B., M. Takemoto, S. Fujibayashi, *et al.* Pore throat size and connectivity determine bone and tissue ingrowth into porous implants: three-dimensional micro-CT based structural analyses of porous bioactive titanium implants. *Biomaterials* 27(35):5892–5900, 2006.
- <sup>31</sup>Pilliar, R. M. Porous-surfaced metallic implants for orthopedic applications. *J. Biomed. Mater. Res.* 21(A1 Suppl):1–33, 1987.
- <sup>32</sup>Ryan, G., A. Pandit, and D. P. Apatsidis. Fabrication methods of porous metals for use in orthopaedic applications. *Biomaterials* 27(13):2651–2670, 2006.
- <sup>33</sup>Shivaram, A., S. Bose, and A. Bandyopadhyay. Thermal degradation of TiO<sub>2</sub> nanotubes on titanium. *Appl. Surf. Sci.* 317:573–580, 2014.
- <sup>34</sup>Shivaram, A., S. Bose, and A. Bandyopadhyay. Damage evaluation of TiO<sub>2</sub> nanotubes on titanium. *Biomater. Sci.* 254:117, 2015.
- <sup>35</sup>Staiger, M. P., M. P. Alexis, H. Jerawala, *et al.* Magnesium and its alloys as orthopedic biomaterials: a review. *Biomaterials* 27:1728–1734, 2006.
- <sup>36</sup>Thieme, M., K. P. Wieters, F. Bergner, *et al.* Titanium powder sintering for preparation of a porous FGM destined as a skeletal replacement implant. *Mater. Sci. Forum* 308:374, 1999.
- <sup>37</sup>Traini, T., C. Mangano, R. L. Sammons, F. Mangano, A. Macchi, and A. Piattelli. Direct laser metal sintering as a new approach to fabrication of an isoelastic functionally graded material for manufacture of porous titanium dental implants. *Dent. Mater.* 24(11):1525–1533, 2008.
- <sup>38</sup>Xue, W., V. K. Balla, A. Bandyopadhyay, and S. Bose. Processing and biocompatibility evaluation of laser processed porous titanium. *Acta Biomater.* 3(6):1007–1018, 2007.
- <sup>39</sup>Yamada, H., and F. G. Evans. *Strength of Biological Materials*. Baltimore, MD: Williams and Wilkins, 1970.
- <sup>40</sup>Yavari, S. A., J. van der Stok, Y. C. Chai, *et al.* Bone regeneration performance of surface-treated porous titanium. *Biomaterials* 35(24):6172–6181, 2014.
- <sup>41</sup>Yue, S., R. M. Pilliar, and G. C. Weatherly. The fatigue strength of porous-coated Ti–6% Al–4% V implant alloy. *J. Biomed. Mater. Res.* 18(9):1043–1058, 1984.